NUMERICAL ANALYSIS OF FUEL MIXING PHYSICS IN GAS TURBINE COMBUSTOR

Harinarayanan Nagarajan[1], Manigandan Rangasamy[2], Murali Kunchi[3], Venkateswararao Boddu[4]
[1]CFD Manager, E&U, Cyient, [2]Team Lead, E&U, Cyient,
[3]FEA Manager, E&U, Cyient, [4]General Manager, E&U, Cyient

Abstract

Combustion physics is a vital challenge for the gas turbine designers. The requirement of reduced emission is in global demand by combustor manufacturers of both aeronautical application and power generation. Due to challenges of cost involved in combustor testing and measurement, it is imperative for a designer to use numerical simulation technique to get insight of the complex physics and ensure better design to meet low emission requirements. Here, attempt is made to investigate the effect of suitability of the numerical models for design analysis on achieving better fuel mixing efficiency on a scaled down model of gas turbine combustor.

Keywords: burner simulation, chemical reaction, turbulent flow, fuel mixing, CFD, RANS

Introduction:

Design of burners in gas turbine combustor play significant role in several industries. The burners need attention to operate at good efficiency while ensuring environment-friendly atmosphere. Stringent emission requirements are making the design of burners very challenging and pollution of combustors make one of the limiting aspects in optimization of the combustor. Numerous studies are in progress to evolve a design which provides low emission of NOx, CO, etc.

In-depth understanding of mixing of fuel species, turbulence, and recirculation are needed to understand the cold flow behaviour of the burner. Study of the lean blow off performance using cold flow analysis by Hu et al [1] showed influence of load parameter (mr.vf) in relevance to burner design. Murlidhara et al [2] showed the simulation of cold flow in a typical annular combustor using commercial CFD code PHOENICS and validation of the predictions with the experimental results. G. K. Caetano et al [3] applied the use of ABAQUS CFD to study the reverse flow type combustor and analysed the mass flow rates, velocity profile with comparison of experimental data. On the other hand, combustion analysis seeks more complicated understanding of chemical reaction, turbulence-chemistry interaction, etc. The hot flow analysis helps analysing the efficiency of combustion, and formation of emissions in detail. Computational fluid dynamics (CFD) is an essential tool to study the physics in relevance to combustion. Measurement of flow behaviour during combustion is extremely difficult and, in such areas, CFD helps significantly to understand the fundamental phenomenon. Dumrongsak et al [4] showed that the predictions of the mixture fraction, velocity by LES method are in agreement with experimental data. It is also emphasized that the results are influenced considerably by the grid resolution. Simulation of chemical kinetics mechanism with CFD is studied on commercial software FLUENT and showcased the usefulness of species transport model in computing temperature, NO, and concentration profiles, by Banger, et al [5]. Chen et al [6] showed the numerical simulation of homogeneous combustion characteristics of methane-air mixtures in micro combustors and they indicated the effect of wall thermal conductivity on controlled combustion thereby on the temperatures and hotspots. The chemical reaction was modelled using species transport and eddy dissipation concept available in FLUENT by Kalla et al [7]. The study confirmed the capability of combustion modelling and validation with experimental data. The phenomenon of NOx formation due to increase in residence time of product combustion gases at higher temperatures are modelled using FLUENT by Lima et al [8].

The correlation of soot formation with fuel composition and temperature are studied by Naegeli et al [9] and also outlined that while soot concentration increased significantly as flame temperature increased, the increase in soot with fuels of lower H/C ratio was much stronger than could be attributed to associated increases in the flame temperature. Colket et al [10] studied experimentally and numerically the soot formation and they used a two-dimensional, detailed soot growth model in which the equations for particle production are coupled to the flow and gaseous species conservation equations has been used to investigate soot production in the flame along with finite rate chemistry model. They found that the radiation losses significantly affected predicted temperatures. Koo et al [11] found that LES simulation captures recirculation zones accurately. Also, the direct relationship between soot volume fraction and equivalence ratio are arrived. Besides, the result of soot field suggests that when secondary oxidation jets are present, inner recirculation region becomes fuel lean and the soot generations are suppressed. Soot field is highly intermittent suggesting that a very restrictive set of gas phase conditions promote soot generation.

In this paper, the model is described initially and then the cold flow analysis results are presented for mesh sensitivity, and different fuel port design using RANS. Subsequently, combustion results are discussed for one of the operating conditions.

Nomenclature:

CFD	Computational Fluid Dynamics
RANS	Reynolds Average Navier Stokes
A*	Pre-exponential Factor
Ea	Activation Energy
A#	Mixing Rate Constant
B#	Mixing Rate Constant
CO	Carbon Monoxide
NOx	Nitro-oxides
i	species

Model Description:

A 3D coaxial burner model is employed for simulation. It contains inlet boundary for air flow, swirler blade in air flow path to provide efficient mixing. Fuel flow is made possible through fuel pipe with nozzle and it mixes with air downstream. The extreme boundary is outlet. All solid boundaries including the swirler blade set are set as wall, assumed to be adiabatic and impermeable. Figure 1 shows the fluid domain employed for the study. The wire frame picture shows the fuel pencil, swirler blade in the combustor, refer Figure 2 Swirler blade ensures circulation to support mixing.

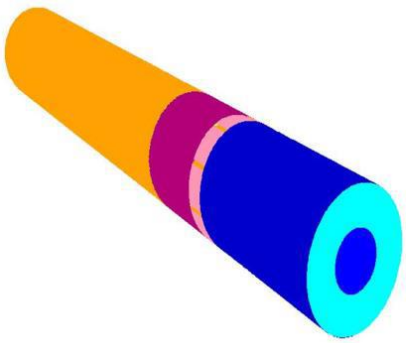

FIGURE 1: FLOW DOMAIN.

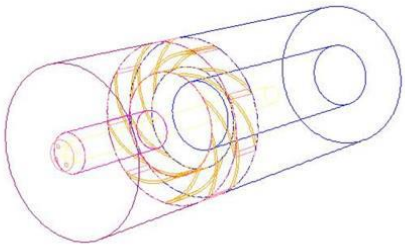

FIGURE 2: WIREFRAME OF THE MODEL.

As shown in Figure 1, the rear extension domain is made longer by five times the diameter of the outer surface to ensure no reverse flow effect in the simulation.

Governing Equation:

The general form of Navier Stokes equation for turbulent flow can be expressed as follows:

$$\frac{\partial(\rho\Phi)}{\partial t}+\frac{\partial}{\partial x_i}\left(\rho U_i\Phi-\Gamma_\Phi\frac{\partial\Phi}{\partial x_i}\right)=q_\Phi \quad (1)$$

where $\Phi=1$, U_j, T, we can respectively get continuity equation, momentum equation and energy equation. The substitution of Φ with T, k, ω, and y yields respectively the equations of energy, turbulent kinetic energy, dissipation rate of turbulence, species transport.

Finite Rate/Eddy Dissipation Model:

The reaction flow simulation is carried out using finite rate/eddy dissipation model. For homogeneous reactions, a combined model of finite rate and eddy dissipation are used together. There model computes both the Arrhenius rate and the eddy dissipation rate and uses the lower of the two.

In the EDC model, the total space is divided into smaller spaces to account for reaction, called fine structures. The reactions are assumed take place in these fine structures. These models are described in more detail in theory guide of the commercial code FLUENT [12]. The net source of chemical species i due to reaction [12] is computed as the sum of the Arrhenius reaction sources over the N_R reactions that the species participate in,

$$R_i = M_{w,i}\sum_{r=1}^{N_R} R_{i,r} \quad (2)$$

Where, $M_{w,i}$ is the molecular weight of species i, $R_{i,r}$ is the Arrhenius molar rate of creation/destruction of species i in reaction r.

$$k_{f,r} = A_r e^{-\frac{Er}{RT}} T^{\beta r} \quad (3)$$

where A_r is pre exponential factor, βr is the temperature exponent, E_r is the activation energy for the reaction (J/kgmol) and R is the universal gas constant (J/kgmol-K).

Numerical Scheme and Grid:

The computational model uses a 3D steady state solver in single precision setup. Least squares cell-based method is used which helps in evaluating gradients. Table 3 summarizes the solver settings. A second order upwind scheme is used for the discretization of conservative equations of species, energy, and momentum. Quantities at the cell faces are determined by assuming that the cell centre values represent an average value and hold throughout the cell [7]. First order upwind scheme is used for turbulence equations. Standard scheme is used for pressure interpolation. Realisable K-epsilon turbulence model [12] is used for simulation.

The numerical grid is constructed as 3D structured mesh. For mesh sensitivity analysis, three different mesh model of 2.05 million cells, 3.02 million cells, 7.43 million cells are made. For detailed analysis with various boundary condition of non-reacting flow and reacting flow, the model of 3.02 million cells is used. Minimum orthogonal quality of all the mesh is ensured to be 0.4 and above. Maximum aspect ratio is ensured to be less than 39.

Simulation Conditions:

All of the simulations are carried out as steady state flow process. In this paper, the simulation is carried out in three different approaches. Firstly, the model is tested for mesh sensitivity with three different type of meshes such as coarse mesh, medium fine mesh and fine mesh. The air inlet boundary condition specified corresponds to a velocity of 14 m/s and fuel inlet boundary condition with velocity of 4.5 m/s specify fuel mixture of methane and ethane with mole fraction of 0.95 and 0.05 respectively. The fuel stream composition is defined by selecting appropriate species and setting their mole fractions. Temperature boundary condition of air is 450 K and fuel is considered as 300 K. The operating pressure of the combustor is 1.8 Mpa. RANS solution is obtained for several design cases in order to study the fuel mixing phenomena which in turn helps in understanding the emission (NOx, CO) formation and also soot formation.

Chemical reaction is carried out using finite rate eddy dissipation method. Chemical kinetics used here is based on a global reduced mechanism, with the following equations:

$$CH_4 + 2O_2 \rightarrow CO_2 + 2H_2O \quad \text{(R1)}$$

$$C_2H_6 + 3.5O_2 \rightarrow 2CO_2 + 3H_2O \quad \text{(R2)}$$

The table 1 below shows the Arrhenius rates used for the reactions,

Reaction	A*	Ea (j/kgmol)	a#	b#
R1	2.119.1011	2.027.108	4	0.5
R2	6.186 .109	1.256.108	4	0.5

TABLE 1: PARAMETERS FOR REACTION.

Results and Discussions:

The computational fluid dynamics calculation for all the design cases in study are carried out using FLUENT version 14.5. Workstation with capacity of 24 cores is employed in the study.

Mesh Sensitivity:

The cold flow results of coarse mesh, refine mesh are compared and it is observed that the results don't vary significantly. Hence, with perspective of time saving, mesh count model of 3 million elements is selected for further study. The Fig 2 shows the velocity plot which were measured downstream of burner. Fig 3 shows the fuel mass fraction pattern in similar fashion as mentioned above.

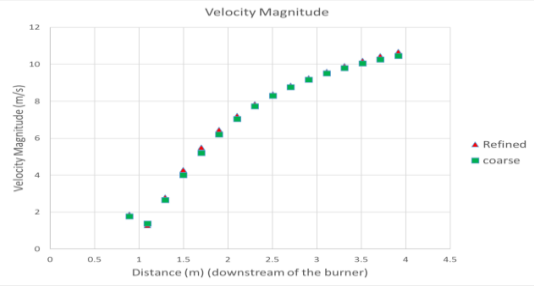

FIGURE 2: VELOCITY CURVE.

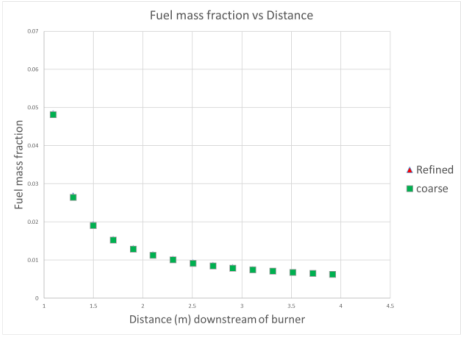

FIGURE 3: FUEL MASS FRACTION CURVE.

Results Without Chemical Reaction:

The cold flow species analysis is carried out using three different designs. Fuel pencil have two ports, three ports, and four ports in three different designs and are referred as design-A, design-B, design-C respectively as shown in Fig 6, 7, 8. The results comparison indicate the design C provides good fuel mixing efficiency. The radial section is made through a section plane several mm down stream of fuel burner and fuel mass fraction contour through radial section shown in Fig 9, 10, 11 indicates species mixing pattern for all designs.

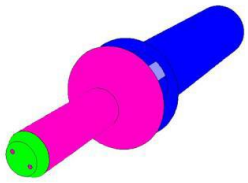

FIGURE 6: TWO FUEL PORT ('A').

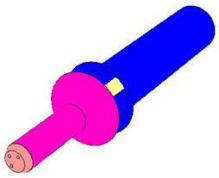

FIGURE 7: THREE FUEL PORT ('B').

FIGURE 8: FOUR FUEL PORT ('C').

The velocity magnitude plot shown in Fig 12, 13, 14 is made using longitudinal plane passing through centre axis of burner. The flow with symmetrical pattern can be observed for design case A and design case C whereas the velocity pattern shows asymmetry in design case B due to geometrical effect.

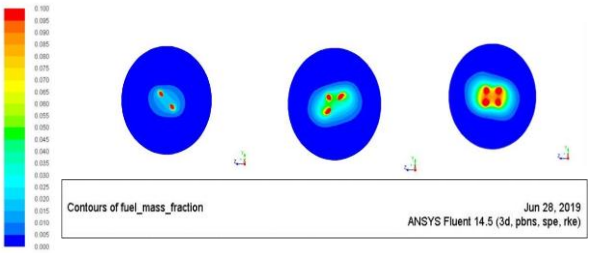

(9) (10) (11)

FIGURE 9: FUEL MASS FRACTION (‘A’).
FIGURE 10: FUEL MASS FRACTION (‘B’).
FIGURE 11: FUEL MASS FRACTION (‘C’).

The results of fuel mass fraction along the longitudinal plane is shown in Fig 15, 16, 17 for the three designs. The plots also indicate symmetrical behaviour for design case (A) and design case (C) and asymmetry in design case (B). The plot is clearly indicating the mixing pattern and efficiency along the flow path downstream of the combustor.

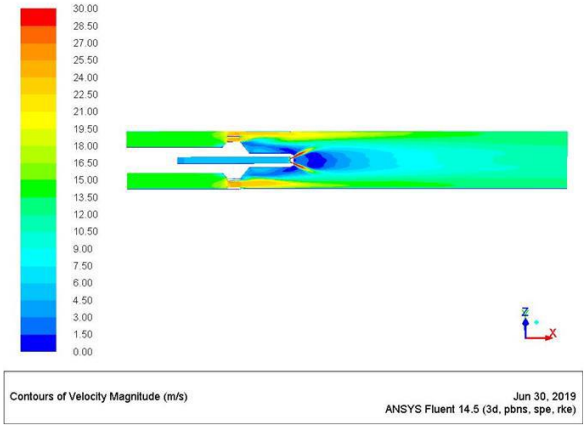

FIGURE 12: VELOCITY MAGNITUDE (‘A’).

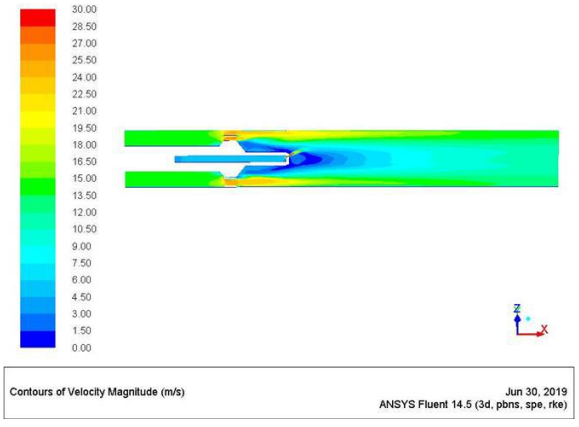

FIGURE 13: VELOCITY MAGNITUDE (‘B’).

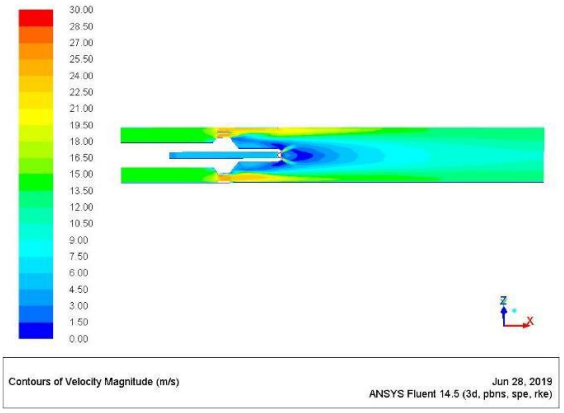

FIGURE 14: VELOCITY MAGNITUDE (‘C’).

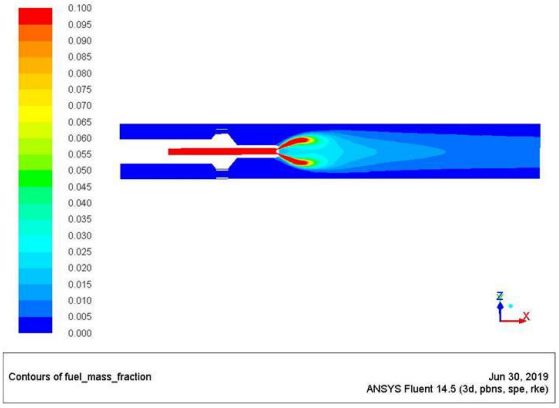

FIGURE 15: FUEL MASS FRACTION (‘A’).

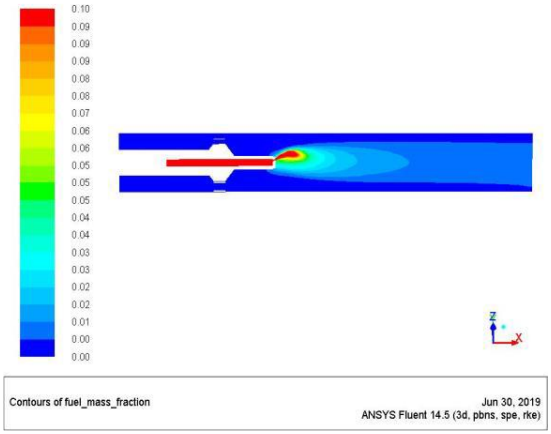

FIGURE 16: FUEL MASS FRACTION (‘B’).

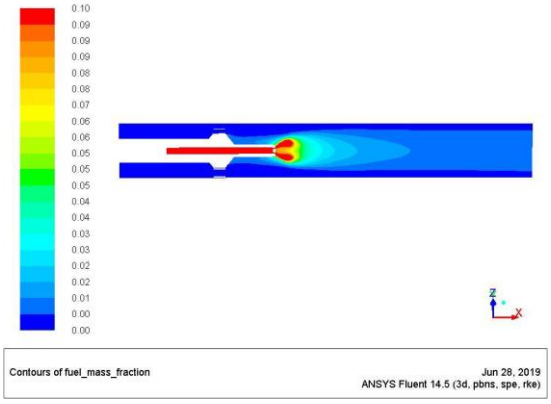

FIGURE 17: FUEL MASS FRACTION (‘C’).

Results with Chemical Reaction:

The chemical reaction calculation is carried out using volumetric reaction concept available in FLUENT software. The temperature contours are made through longitudinal section plane for all three cases and the combustion results show the temperature rise in the combustor for all design cases, as per Arrhenius equation for the given equivalence ratio and reaction constants. Temperature contour show symmetrical behaviour for design (A) and design (C).

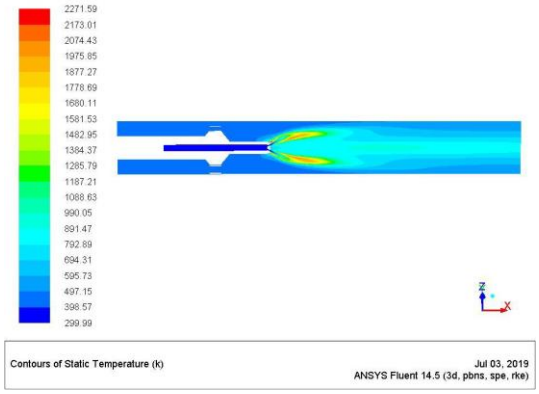

FIGURE 18: STATIC TEMPERATURE ('A').

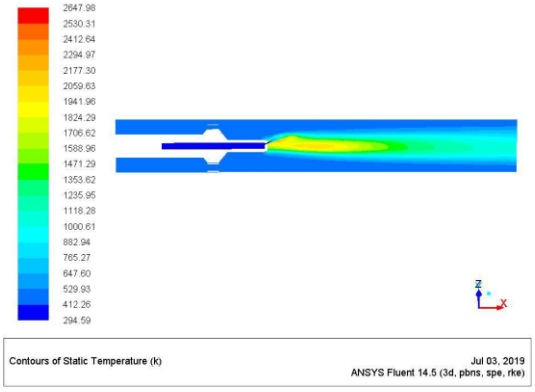

FIGURE 19: STATIC TEMPERATURE ('B').

The results are in line with the contours shown in paper by Dumrongsak, et al [4] and Chen, et al [6]. Symmetric flame by RANS method is as expected, refer Fig 18 and Fig 20. Asymmetric flame of design case (B) is due to geometrical limitation, refer Fig 19.

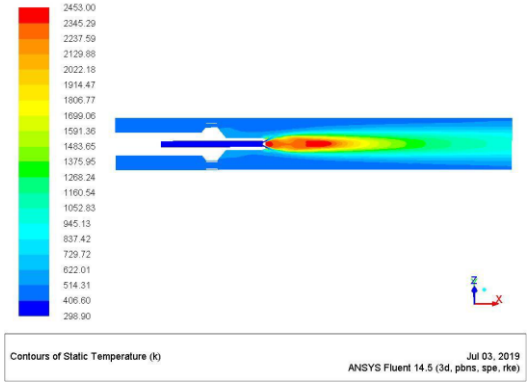

FIGURE 20: STATIC TEMPERATURE ('C').

Corresponding product mass fraction contour plots are shown in Fig 21, 22 and 23. More products can be seen near the upstream region in proximity to burner fuel port than the downstream region which is consistent with mixture fraction predictions. Empirical relation of the mass fraction also indicates the region of soot formation similar to the pattern shown in Fig 23.

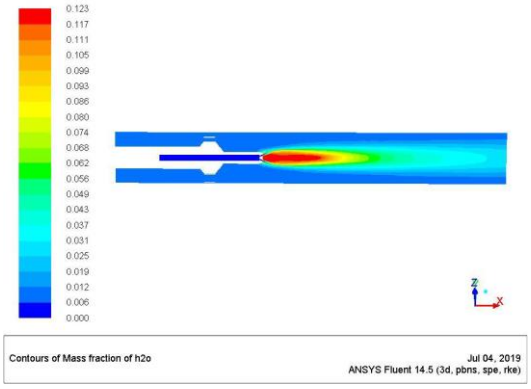

FIGURE 21: PRODUCT MASS FRACTION ('C').

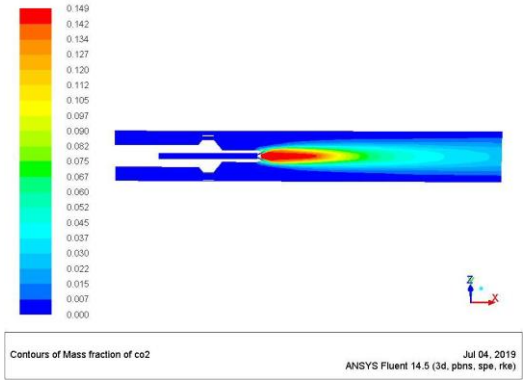

FIGURE 22: PRODUCT MASS FRACTION ('C').

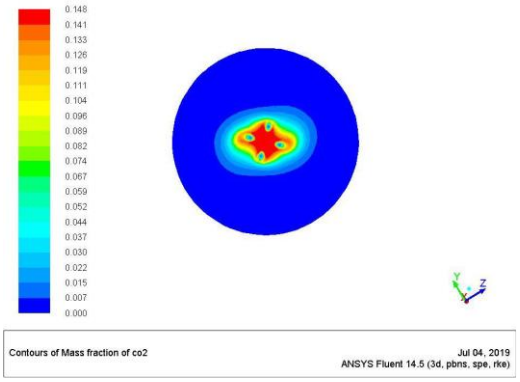

FIGURE 23: STATIC TEMPERATURE ('C').

Conclusions:

The cold flow analysis of combustor is studied for several design and the results showed the design which provide best fuel mixing efficiency. Fuel mass fraction of the combustor downstream of the burner port showed the mixing pattern decays with distance. Combustion characteristics of the three designs are also successfully accomplished using commercial software FLUENT. The results using RANS simulation showed similar pattern as observed by past researchers. The combustion results obtained from methane-ethane fuel shows good mixing and reaction for design 'C'. Contours of products and fuel mass fraction indicate the region of soot formation which are confirmed through simple empirical equation method. Research will be continued in future with more detailed soot model and also using LES method.

Acknowledgements:

The authors would like to acknowledge energy (E&U) business unit of CYIENT for supporting this study. Author appreciates the effort of Manigandan R for supporting in flow domain preparation, mesh generation and post processing plot preparation. Author also expresses sincere thanks to Suresh Nagarowth, vice president, E&U of CYIENT for the encouragement.

References:

[1] Bin Hu, Yong Huang, Fang Wang and Fa Xie, (2011), Numerical Simulation of Cold Flow Field of AeroEngine Combustors for Lean Blow Off Analysis, ASME 2011 Turbo Expo: Turbine Technical Conference and Exposition, Volume 2: Combustion, Fuels and Emissions, Parts A and B, 477-484

[2] Hs, Muralidhara & Shembharkar, TR & Pai, BR & Ramanujam, PS & Jayaprakash, GN & Pandey, PK. (2001). Cold flow analysis of an aero-engine gas turbine combustor configuration, International symposium of Air Breathing Engines.

[3] Caetano, G.K, Carvalho, J. F. T. de, Rosa, J.S. (2019), Cold flow numerical analysis of gas microturbine combustion chamber through cfd tool, Engenharia Térmica (Thermal Engineering), Vol. 18 • No. 1 • June 2019 • p. 29-35

[4] Dumrongsak J, and Savill A.M. (2012), Numerical analysis and sensitivity study of non-premixed combustion using LES, International scholarly and scientific research & innovation 6(12) 2012, 2770-2781.

[5] Banger, Nikita, and Dr. Prasad, S. (2015), Study of natural gas combustor using species transport model, International Journal of computer & mathematical sciences, Vol 4, Issue 2, 40-43.

[6] Chen, Junjie and Song, Wenya, (2015), Homogeneous combustion characteristics of premixed methane-air mixtures in micro-combustors, J. of physical and chemical sciences, vol3/issue4, 1-6.

[7] Kalla, Smail, Marcoux, Hugo, and deChamplain, Alain, (2015), CFD approach for modeling high and low combustion in a natural draft residential wood log stove, International journal of heat and technology, vol22, no1, 33- 38.

[8] Lima, Rodrigo C. R., Nogueira, Manoel F. M., and Guerra, Danielle R. S., (2017), CFD modeling of a smallscale cyclonic combustor chamber using biomass powder, Energy procedia 120, 556-563.

[9] Naegeli, David W., Dodge, Lee G. & Moses, Clifford A. (1983), Effects of Flame Temperature and Fuel Composition on Soot Formation in Gas Turbine Combustors, Combustion Science and Technology, 35:1-4,117131, DOI: 10.1080/00102208308923706

[10] Colket, Meredith B., Hall, Robert J., Liscinsky, David S., and Smooke, Michell D., (1998), Fundamentals of Soot Formation in Gas Turbine Combustors, UTRC98-5.100.0016-1.

[11] Koo, Heeseok., Hassanaly, Malik., Raman, Venkat., Mueller, Michael E., and Geigle, Klaus Peter, (2016), Large-Eddy Simulation of Soot Formation in a Model Gas Turbine Combustor, J. Eng. Gas Turbines Power 139(3), 031503 (Sep 27, 2016) (9 pages)

[12] FLUENT 14.5 User's Guide, (2009), Fluent Inc., chapter 7.1, and chapter 4, pp 4-1 to 4-88